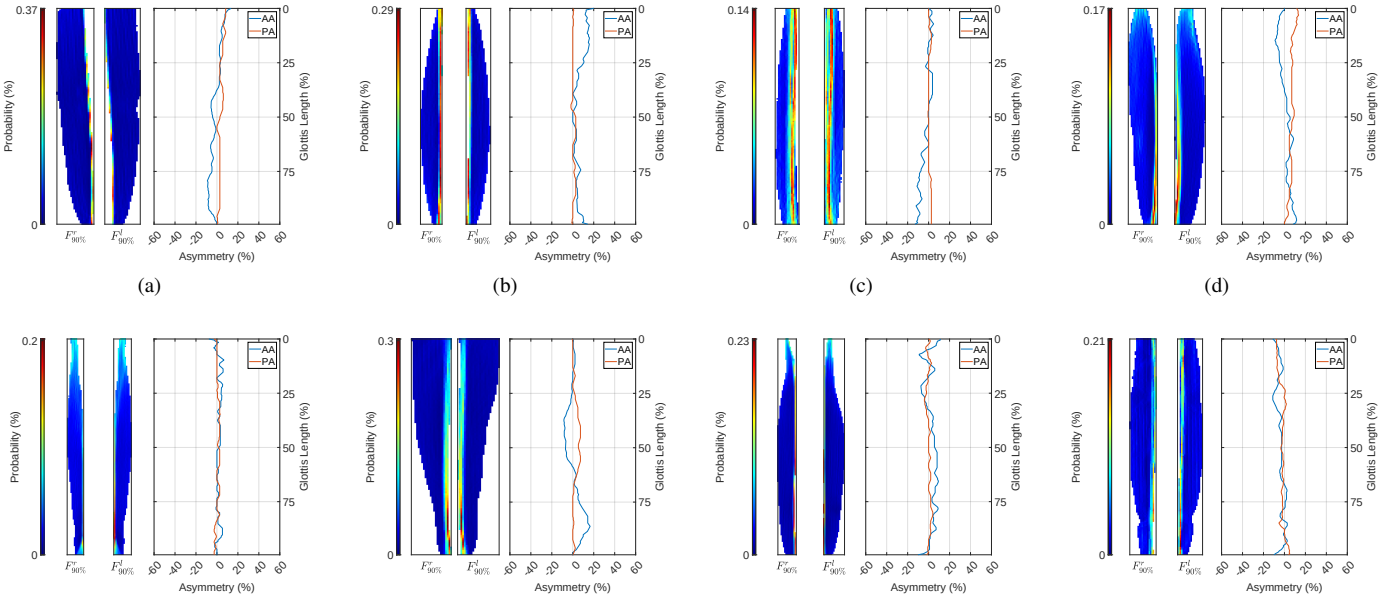

Fig. 1: Assessment of vibratory asymmetry in normal subjects. The panels depict the effective displacement range of the individual empirical distributions for the right ($F^{\mathtt{r}}(x,y)$) and left ($F^{\mathtt{l}}(x,y)$) edges, along with the characterization of Amplitude Asymmetry (AA) and Phase Asymmetry (PA) along the anterior-posterior dimension. Participants with typical voices: (a) FN09, (b) FN10, (c) FN11, (d) FN12, (e) FN13, (f) FN14, (g) FN15, and (h) MN16. The color maps represent the empirical probability as a percentage.

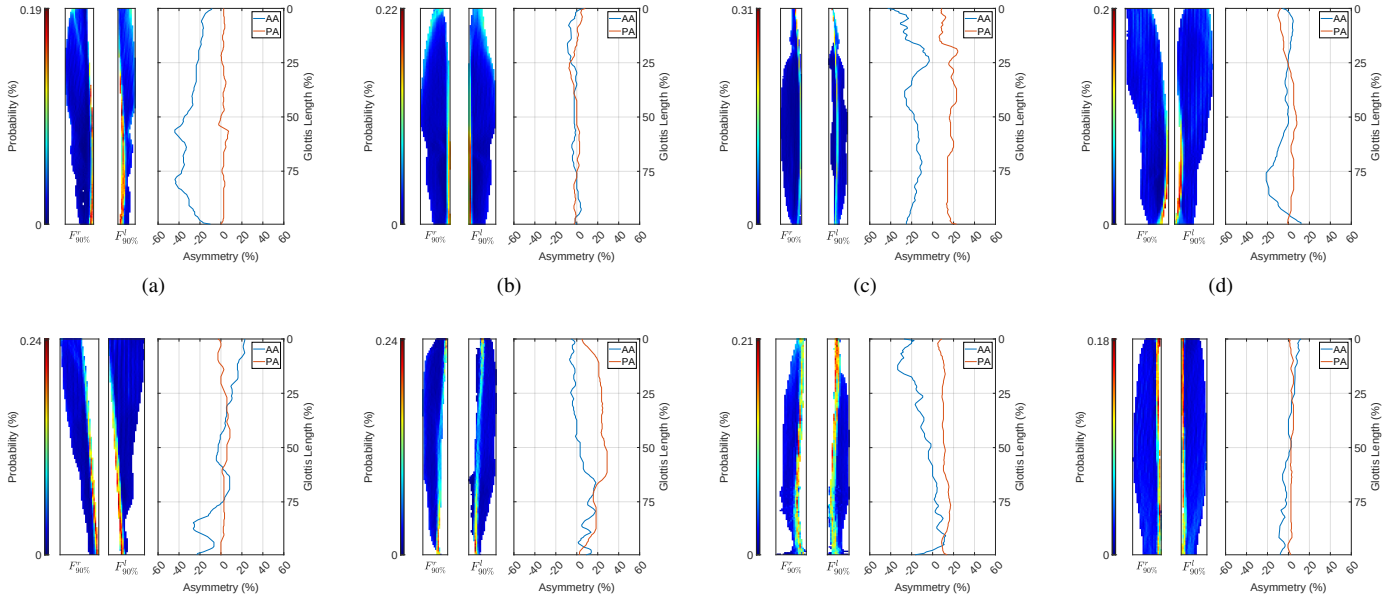

Fig. 2: Assessment of vibratory asymmetry in MTD patients. The panels depict the effective displacement range of the individual empirical distributions for the right ($F^{\mathrm{r}}(x,y)$) and left ($F^{\mathrm{l}}(x,y)$) edges, alongside the characterization of Amplitude Asymmetry (AA) and Phase Asymmetry (PA) along the anterior-posterior dimension. Participants with typical voices: (a) FP17, (b) FP18, (c) FP19, (d) FP20, (e) FP21, (f) MP22, (g) MP23, and (h) MP24. The color maps represent the empirical probability as a percentage.

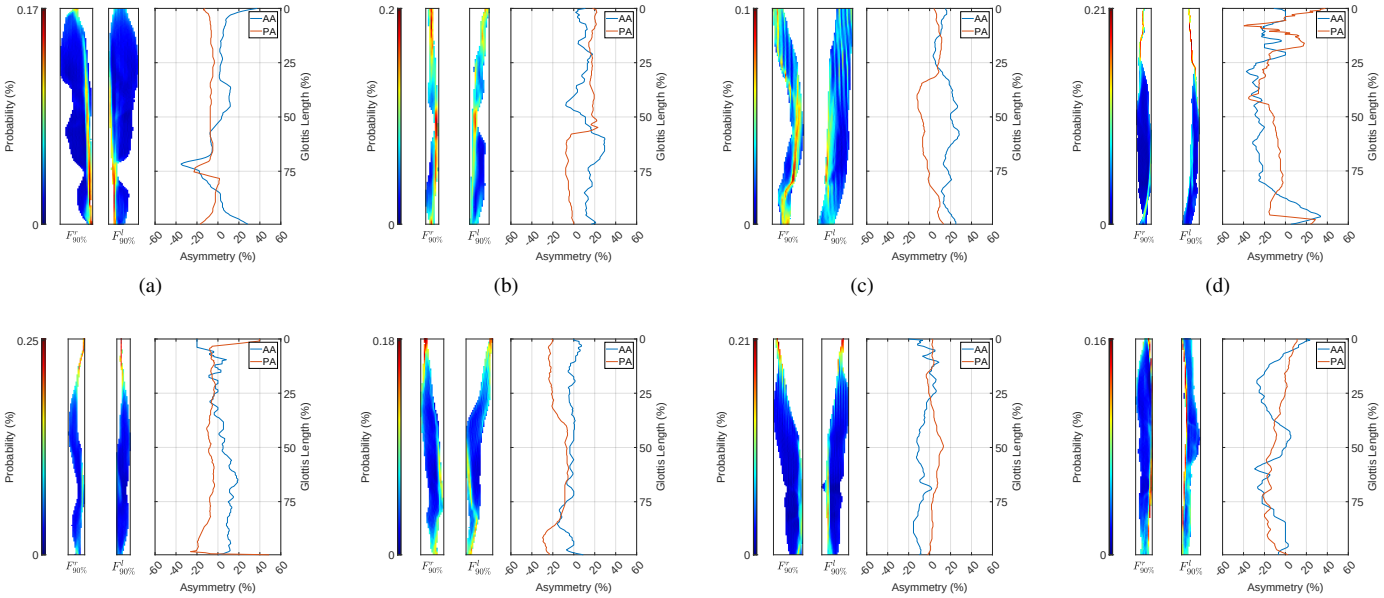

Fig. 3: Assessment of vibratory asymmetry in patients with bilateral nodules. The panels depict the effective displacement range of the individual empirical distributions for the right ($F^{\mathtt{r}}(x,y)$) and left ($F^{\mathtt{l}}(x,y)$) edges, alongside the characterization of Amplitude Asymmetry (AA) and Phase Asymmetry (PA) along the anterior-posterior dimension. Participants with typical voices: (a) FP25, (b) FP26, (c) FP27, (d) FP28, (e) FP29, (f) FP30, (g) FP31, and (h) MP32. The color maps represent the empirical probability as a percentage.